# SUPPLEMENTARY INFORMATION

## Nanoscale glucan polymer network causes pathogen resistance

Dennis Eggert[1,2,*], Marcel Naumann[3,*], Rudolph Reimer[1], Christian A. Voigt[3,‡]

[1]Microscopy and Image Analysis Group, Heinrich-Pette-Institute, Leibniz Institute for Experimental Virology, Hamburg
[2]Institute of Physical Chemistry, University of Hamburg, Hamburg, Germany
[3]Phytopathology and Biochemistry, Biocenter Klein Flottbek, University of Hamburg, Hamburg, Germany
[*]These authors contributed equally to this work.
[‡]Corresponding author e-mail: christian.voigt@uni-hamburg.de

**CONTENT**

**Supplementary Figures** **page**

**Supplementary Video Legends** **page**

**Supplementary Figures**

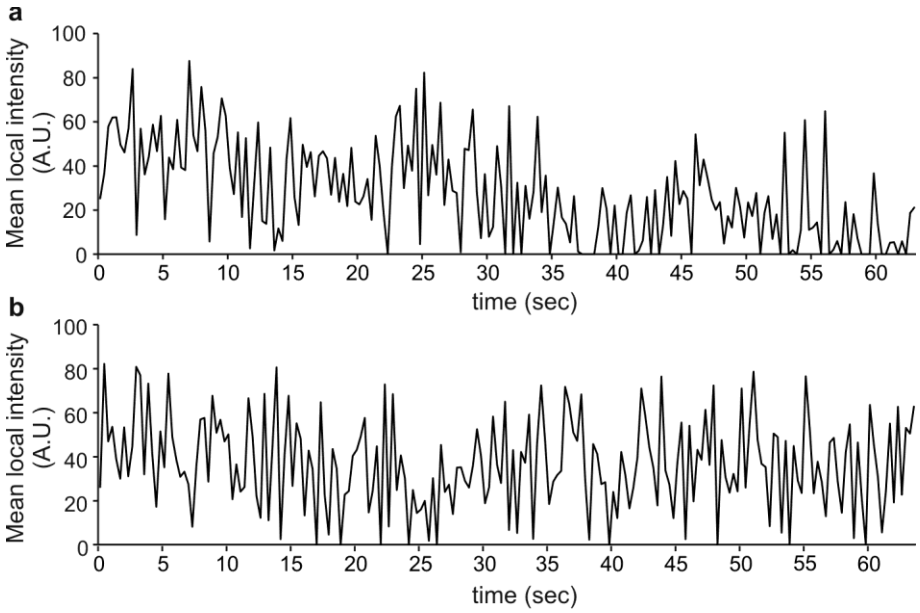


**Figure S1: Intensity fluctuations and photoblinking of the organic fluorophores aniline blue fluorochrome and pontamine fast scarlet 4B.**

Shown is the mean integrated intensity of the fluorescence signal of **a**, aniline blue fluorochrome (ABF) and **b**, pontamine fast scarlet 4B (S4B) after background subtraction vs. time. The off times of the fluorophore are in the range from msec to sec. making it possible to localise diffraction limited spots that represent the signal of single ABF and S4B fluorophores. For the analysis, a region in the size of a single diffraction limited signal (7 x 7 camera pixel) was chosen.

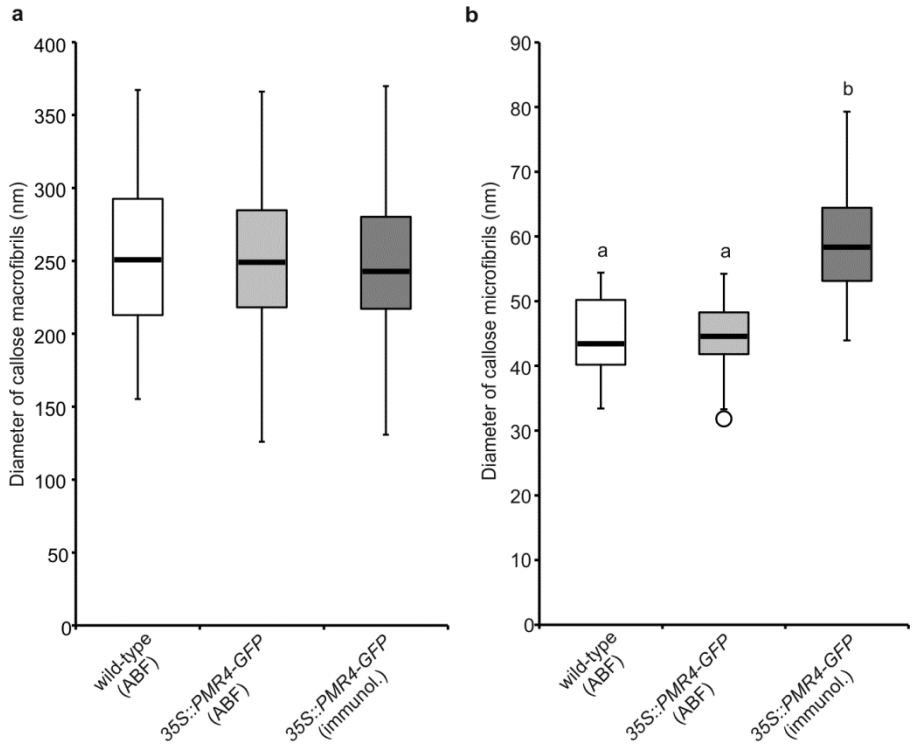


**Figure S2: Diameter of callose macro- and microfibrils in callose deposits at sites of attempted fungal penetration.**

*A. thaliana* wild-type and pathogen-resistant *PMR4*-overexpressing lines (*35S::PMR4-GFP*) were inoculated with *G. cichoracearum*. Visualisation of callose macro- and microfibrils by localization microscopy of aniline blue fluorochrome (ABF)-stained and immunolabelled (immunol.) callose deposits in epidermal leaf cells at 6 h post-inoculation. **a**, Diameter of callose macrofibrils. **b**, Diameter of callose microfibrils. Box plots from $n = 50$ measurements of four individual plants, whiskers: minimum and maximum value within the 1.5 x interquatrile range (IQR), circle: outlier outside the 1.5 x IQR. a, b: $P < 0.001$ Tukey's test.

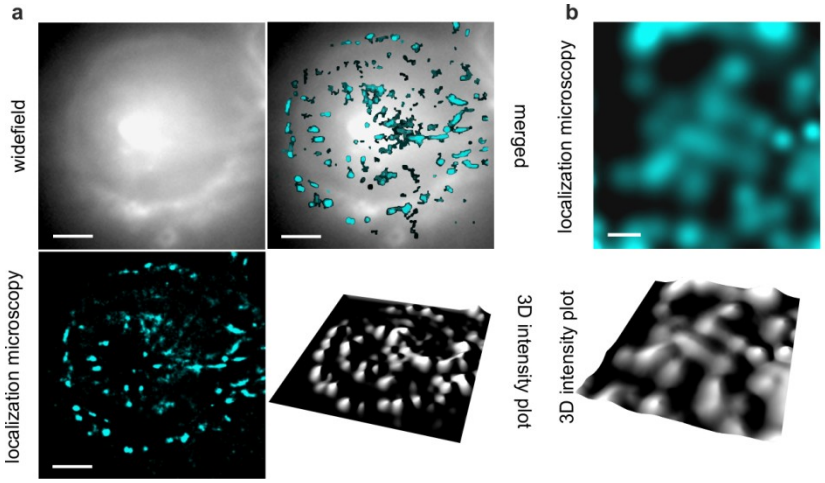


**Figure S3: Nanoscale resolution of immunolabelled callose polymer fibrils in pathogen-induced cell wall deposits.**

*A. thaliana* pathogen-resistant *PMR4*-overexpressing lines (*35S::PMR4-GFP*) were inoculated with the adapted powdery mildew *G. cichoracearum*. Localisation microscopy was performed with a Zeiss PS.1 super-resolution system. For immunolabelling, a specific anti-callose antibody was used in combination with a CAGE552-coupled secondary antibody. 3D intensity plots highlight orientation and network formation of callose fibrils. **a**, Overview of callose macrofibril orientation. Radial and circular macrofibril orientation in the field of callose of deposits from pathogen-resistant *PMR4*-overexpressing lines resembled orientation of aniline blue fluorochrome (ABF)-stained callose macrofibrils of the same lines (compare with Fig. 1e). Scale bars = 2 µm. **b**, Immunolabelled callose microfibrils revealed similar nanoscale network formation as ABF-stained microfibrils of the same pathogen-resistant lines and wild-type (compare with Fig. 1f). Scale bars = 50 nm.

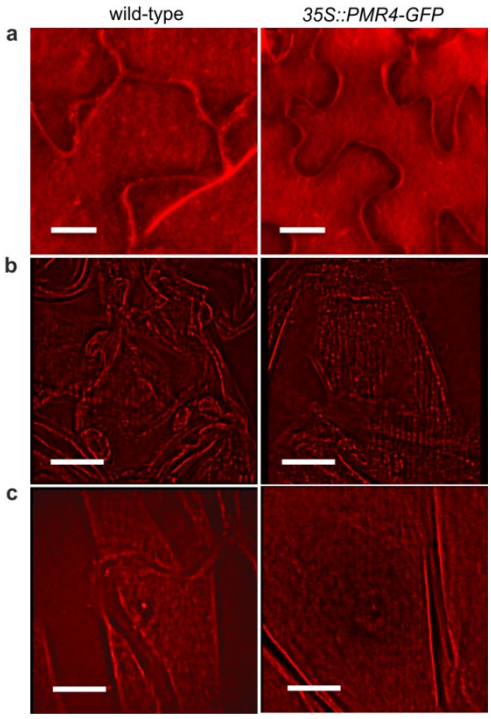


**Figure S4: Establishing localisation microscopy of pontamine fast scarlett 4B stained cellulose macrofibrils.**

Unchallenged rosette leaves of *A. thaliana* wild-type and pathogen-resistant *PMR4*-overexpressing lines (*35S::PMR4-GFP*) were stained with the cellulose-specific dye pontamine fast scarlet 4B. **a**, High-resolution micrographs of epidermal cells taken by confocal laser-scanning microscopy (see also Supplementary Videos 3 and 4). Scale bars = 10 µm. **b**, Localisation microscopy of internal cellulosic cell walls layers. **c**, Localisation microscopy of the cellulosic cell wall surface. Scale bars = 10 µm.

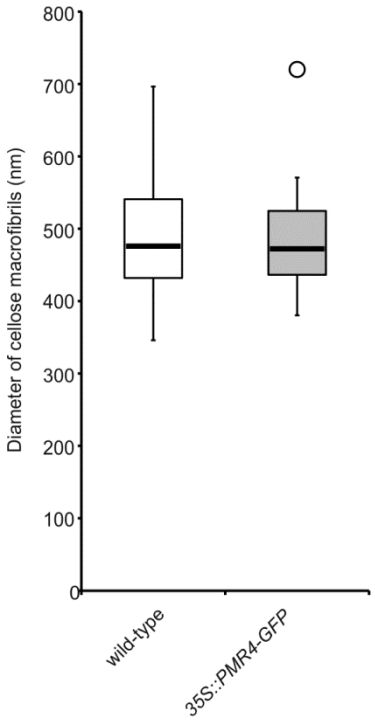


**Figure S5: Diameter of cellulose macrofibrils.**

*A. thaliana* wild-type and pathogen-resistant *PMR4*-overexpressing lines (*35S::PMR4-GFP*) were stained with cellulose-specific dye pontamine fast scarlet 4B. Determination of the diameter of (1,4)-*β*-glucan macrobrils after localisation microscopy of epidermal leaf cells. Box plots from $n$ = 50 measurements of four individual plants, whiskers: minimum and maximum value within the 1.5 x interquatrile range (IQR).

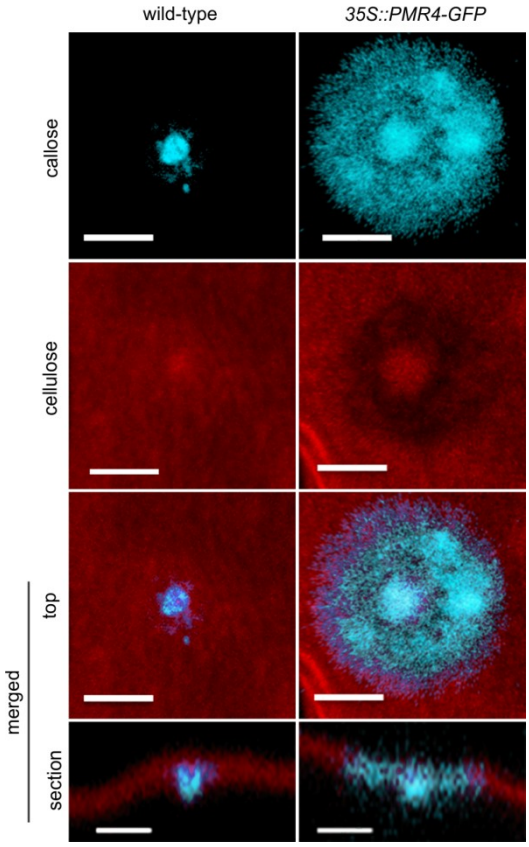


**Figure S6: Interaction of the glucan cell wall polymers callose and cellulose at sites of attempted fungal penetration.**

*A. thaliana* wild-type and pathogen-resistant *PMR4*-overexpressing lines (*35S::PMR4-GFP*) were inoculated with *G. cichoracearum*. Micrographs taken by confocal laser-scanning microscopy at sites of attempted fungal penetration of co-stained epidermal cells. Blue channel: fluorescence of aniline blue fluorochrome (ABF)-stained callose, red channel: fluorescence of pontamine fast scarlet 4B (S4B)-stained cellulose. In silico cross section of pathogen-induce callose deposits and neighbouring cellulosic cell wall showed putative callose/cellulose polymer interaction (lower panels). Scale bars = 5 µm.

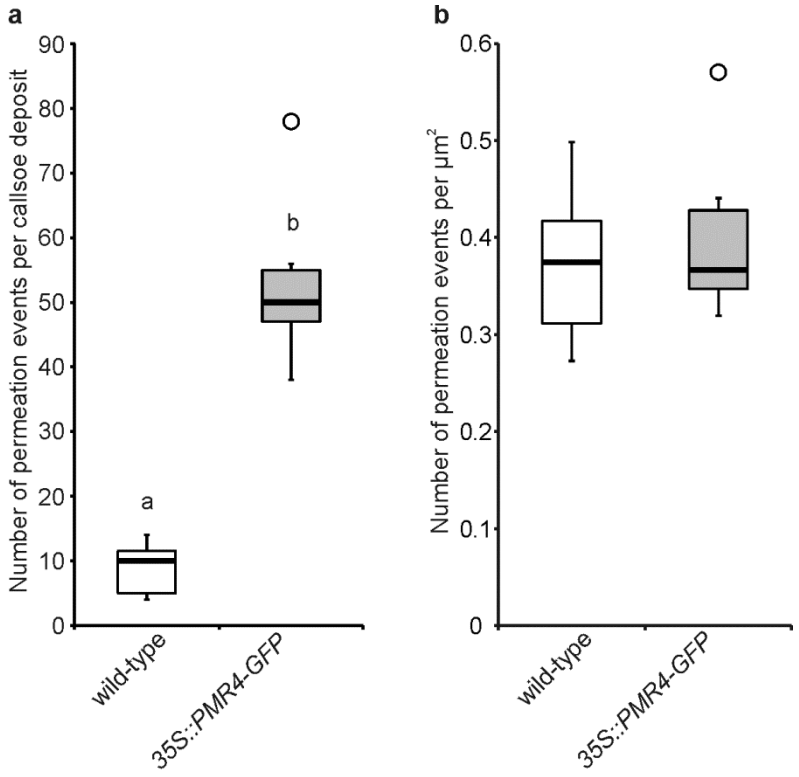


**Figure S7: Number of permeation events of callose fibrils through cellulosic cell wall layers.**

*A. thaliana* wild-type and pathogen-resistant *PMR4*-overexpressing lines (*35S::PMR4-GFP*) were inoculated with *G. cichoracearum*. Localization microscopy was performed at interphases of pathogen-induced callose deposits and the pre-existing cellulosic cell wall (see also schematic overview in Fig. 3) of co-stained epidermal cells. Blue channel: fluorescence of aniline blue fluorochrome (ABF)-stained callose, red channel: fluorescence of pontamine fast scarlet 4B (S4B)-stained cellulose. **a**, Number of callose fibrils permeating cellulosic cell wall layers within the range of a callose deposit was manually counted after imaging. **b**, Density of callose permeation events within the range of a callose deposit. Box plots from $n$ = 10 callose/cellulose interphase sites of three individual plants, whiskers: minimum and maximum value within the 1.5 x interquatrile range (IQR), circle: outlier outside the 1.5 x IQR. a, b: $P < 0.001$ Tukey's test.

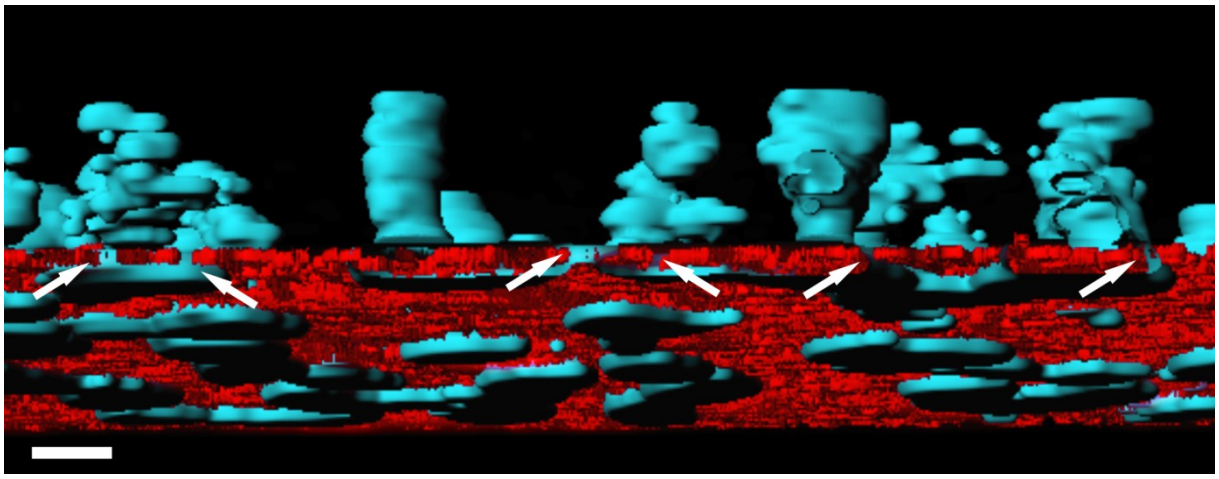

**Figure S8: Permeation of cellulosic cell wall layer by callose fibrils through nanopores.**

*A. thaliana* pathogen-resistant *PMR4*-overexpressing lines (*35S::PMR4-GFP*) were inoculated with *G. cichoracearum*. Localisation microscopy of Co-stained epidermal cells.: Blue channel: fluorescence of aniline blue fluorochrome-stained callose, red channel: fluorescence of pontamine fast scarlet 4B-stained cellulose.. Micrograph shows 3D surface rendered, in silico cross section at the interphase of the callose deposit and the cellulosic cell wall. Arrows indicate possible nanopores as permeation sites of callose fibrils through the cellulosic cell wall layer. Localisation microscopy of the interphase of the callose deposit and the cellulosic cell wall in infected wild-type epidermal leaf cells gave similar results. Scale bar = 200 nm.

## Supplementary Video Legends

**Video S1: Powdery mildew-induced callose deposit in *A. thaliana* wild-type.**

*A. thaliana* wild-type was inoculated with *G. cichoracearum*. High-resolution Z-series of aniline blue fluorochrome-stained callose deposits taken 6 h post-inoculation by confocal laser-scanning microscopy. Video generation from maximum intensity reconstruction and 3D surface rendering using integral functions of the ZEN 2010 (Zeiss GmbH) operating software.

**Video S2: Powdery mildew-induced callose deposit in penetration-resistant *A. thaliana PMR4*-overexpressing line.**

*A. thaliana* pathogen-resistant *PMR4*-overexpressing line (*35S::PMR4-GFP*) was inoculated with *G. cichoracearum*. High-resolution Z-series of aniline blue fluorochrome-stained callose deposits taken 6 h post-inoculation by confocal laser-scanning microscopy. Video generation from maximum intensity reconstruction and 3D surface rendering using integral functions of the ZEN 2010 (Zeiss GmbH) operating software.

**Video S3: Cellulosic cell wall of unchallenged *A. thaliana* wild-type epidermal leaf cells.**

Unchallenged *A. thaliana* wild-type leaves were stained with pontamine fast scarlet 4B to visualise cellulose. High-resolution Z-series taken by confocal laser-scanning microscopy. Video generation from maximum intensity reconstruction using integral functions of the ZEN 2010 (Zeiss GmbH) operating software.

**Video S4: Cellulosic cell wall of unchallenged epidermal leaf cells of the *A. thaliana PMR4*-overexpressing line.**

Unchallenged *A. thaliana* pathogen-resistant *PMR4*-overexpressing line (*35S::PMR4-GFP*) leaves were stained with pontamine fast scarlet 4B to visualise cellulose. High-resolution Z-series taken by confocal laser-scanning microscopy. Video generation from maximum intensity reconstruction using integral functions of the ZEN 2010 (Zeiss GmbH) operating software.

**Video S5: Powdery mildew-induced callose deposit at the cellulosic cell wall in *A. thaliana* wild-type.**

*A. thaliana* wild-type was inoculated with *G. cichoracearum*. High-resolution Z-series of epidermal leaf cells co-stained with aniline blue fluorochrome for callose and pontamine fast scarlet 4B for cellulose taken 6 h post-inoculation by confocal laser-scanning microscopy. Video generation from maximum intensity reconstruction using integral functions of the ZEN 2010 (Zeiss GmbH) operating software.

**Video S6: Powdery mildew-induced callose deposit at the cellulosic cell wall in pathogen-resistant *A. thaliana PMR4*-overexpressing line.**

*A. thaliana* pathogen-resistant *PMR4*-overexpressing line (*35S::PMR4-GFP*) was inoculated with *G. cichoracearum*. High-resolution Z-series of epidermal leaf cells co-stained with aniline blue fluorochrome for callose and pontamine fast scarlet 4B for cellulose taken 6 h post-inoculation by confocal laser-scanning microscopy. Video generation from maximum intensity reconstruction using integral functions of the ZEN 2010 (Zeiss GmbH) operating software.

**Video S7: Permeation of callose fibrils at the cellulosic cell wall interphase in *A. thaliana* wild-type.**

*A. thaliana* wild-type was inoculated with *G. cichoracearum*. 3D Super-resolution imaging of epidermal leaf cells co-stained with aniline blue fluorochrome for callose and pontamine fast scarlet 4B for cellulose taken 6 h post-inoculation by localisation microscopy. Video generation with Bitplane Imaris 7.6.1. (Bitplane).

**Video S8: Permeation of callose fibrils at the cellulosic cell wall interphase in pathogen-resistant *A. thaliana PMR4*-overexpressing line.**

*A. thaliana* pathogen-resistant *PMR4*-overexpressing line (*35S::PMR4-GFP*) was inoculated with *G. cichoracearum*. 3D Super-resolution imaging of epidermal leaf cells co-stained with aniline blue fluorochrome for callose and pontamine fast scarlet 4B for cellulose taken 6 h post-inoculation by localisation microscopy. Video generation with Bitplane Imaris 7.6.1. (Bitplane).

**Video S9: Permeation of callose fibrils at the cellulosic cell wall surface in *A. thaliana* wild-type.**

*A. thaliana* wild-type was inoculated with *G. cichoracearum*. 3D Super-resolution imaging of epidermal leaf cells co-stained with aniline blue fluorochrome for callose and pontamine fast scarlet 4B for cellulose taken 6 h post-inoculation by localisation microscopy. Video generation with Bitplane Imaris 7.6.1. (Bitplane).

**Video S10: Permeation and layer formation of callose fibrils at the cellulosic cell wall surface in pathogen-resistant *A. thaliana PMR4*-overexpressing line.**

*A. thaliana* pathogen-resistant *PMR4*-overexpressing line (*35S::PMR4-GFP*) was inoculated with *G. cichoracearum*. 3D Super-resolution imaging of epidermal leaf cells co-stained with aniline blue fluorochrome for callose and pontamine fast scarlet 4B for cellulose taken 6 h post-inoculation by localisation microscopy. Video generation with Bitplane Imaris 7.6.1. (Bitplane).